Observation of Coherent Coupling between Super- and Subradiant States of an Ensemble of Cold Atoms Collectively Coupled to a Single Propagating Optical Mode

Riccardo Pennetta,* Daniel Lechner, Martin Blaha, Arno Rauschenbeutel, Philipp Schneeweiss, and Jürgen Volz†
Department of Physics, Humboldt Universität zu Berlin, 12489 Berlin, Germany

(Received 22 December 2021; accepted 8 April 2022; published 17 May 2022)

We discuss the evolution of the quantum state of an ensemble of atoms that are coupled via a single propagating optical mode. We theoretically show that the quantum state of N atoms, which are initially prepared in the timed Dicke state, in the single excitation regime evolves through all the $N-1$ states that are subradiant with respect to the propagating mode. We predict this process to occur for any atom number and any atom-light coupling strength. These findings are supported by measurements performed with cold cesium atoms coupled to the evanescent field of an optical nanofiber. We experimentally observe the evolution of the state of the ensemble passing through the first two subradiant states, leading to sudden, temporary switch-offs of the optical power emitted into the nanofiber. Our results contribute to the fundamental understanding of collective atom-light interaction and apply to all physical systems, whose description involves timed Dicke states.

DOI: 10.1103/PhysRevLett.128.203601

The collective interaction of N quantum emitters with light can differ substantially depending on whether the distance between any two of the emitters is significantly smaller or larger than the wavelength of the light field. The former situation has been initially investigated by Dicke [1], who decomposed the Hilbert space of the system in superradiant states, whose decay rates toward lower energy states are enhanced with respect to the decay rates one of an isolated emitter, and subradiant states, for which decay to the ground state is suppressed. In particular, in the single excitation limit which we consider throughout this Letter, the Dicke model identifies a single superradiant state with an N times enhanced decay rate, while there are $N-1$ subradiant states.

A formal description of the time evolution of extended ensembles of emitters (i.e., interatomic distance between any two emitters $> \lambda$) within the same framework of the Dicke model requires the introduction of the so-called timed Dicke states [2], which can be prepared, e.g., by exciting the emitters with a single photon with wave vector $\boldsymbol{k}$:

$$|\mathrm{TD}\rangle = \frac{1}{\sqrt{N}} \sum_{n=1}^{N} e^{i\boldsymbol{k}\cdot\boldsymbol{r}_n} \hat{\sigma}_n^+ |0\rangle. \tag{1}$$

Here, $\boldsymbol{r}_n$ and $\hat{\sigma}_n^+$ indicate the position and the raising operator for the nth emitter in the ensemble and $|0\rangle = |0_{\mathrm{ph}}\rangle \otimes |g_1, \ldots, g_N\rangle$, where $|0_{\mathrm{ph}}\rangle$ is the vacuum state and $|g_1, \ldots, g_N\rangle$ indicates that all atoms are in the ground state. An ensemble in the timed Dicke state experiences superradiant decay and collectively enhanced emission of light into the same optical mode that excited the system. Likewise, it is possible to introduce $N-1$ states, that are orthogonal to the timed Dicke state and subradiant with respect to the optical mode with wave vector $\boldsymbol{k}$. This approach is suitable for describing a considerable number of physical systems, including, for instance, cold atom clouds [3–10], Rydberg atoms [11,12], and emitters in solid-state samples [13]. In addition, in cavity quantum electrodynamics the timed Dicke physics is at the basis of the assumptions of the Tavis-Cummings model [14,15], which describes collectively enhanced light-matter coupling between an atomic ensemble and a single-mode cavity [16,17]. For these reasons, notable effort has recently been devoted to describe the time dynamics of extended ensembles [2,18–22], a task which, unlike the standard Dicke model, needs to consider coupling between super- and subradiant states; see Fig. 1(a).

In this Letter, we study a one-dimensional ensemble of atoms coupled via a single optical mode, and we discuss the time evolution of its state. We present a theoretical approach that unveils the microscopic temporal dynamics of the system within a simple mathematical framework. We show that during its temporal evolution, an ensemble initially prepared in the timed Dicke state evolves through all basis states of the Hilbert space, reaching, one after the other, all the $N-1$ subradiant states. This process occurs for any atom number (unlike the case of three-dimensional

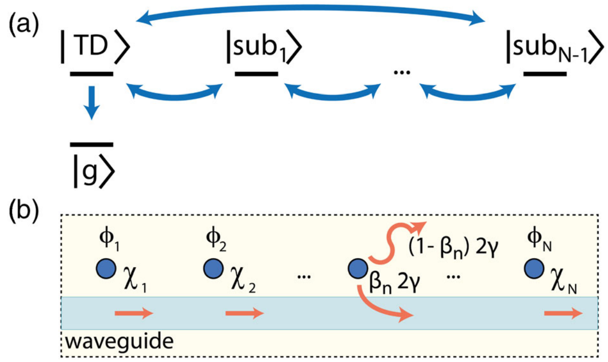

FIG. 1. (a) Collective states for an ensemble of N atoms in the single excitation limit. TD, timed Dicke state; sub$_n$, nth subradiant state; g, ground state. (b) N atoms coupled to a single-mode optical waveguide. The factors $\beta_n\, 2\gamma$ and $(1-\beta_n)2\gamma$ represent the photon emission rate of the nth atom into guided and unguided optical modes, respectively. The excited state amplitude of the nth atom is indicated by ϕ_n, while χ_n is the light field amplitude right after the nth atom.

atom clouds [18]) and for any coupling strength. Notably, it already appears for two emitters with arbitrarily weak coupling to the optical mode [23]. To support the predictions of our model, we present experimental results that we obtain interfacing an ensemble of cold cesium (Cs) atoms with the evanescent field part of the guided mode of an optical nanofiber. After exciting the atoms with boxcar-shaped nanofiber-guided laser pulses with a switch-off time much shorter than the atomic lifetime, we investigate the temporal response of the system by recording the optical power exiting the nanofiber. We observe the passage of the state of the ensemble through the first two subradiant states with respect to the guided mode, which leads to abrupt and temporary drops in the nanofiber-guided light field.

A sketch of the considered configuration is shown in Fig. 1(b). An ensemble of N atoms is coupled to a single guided optical mode. The atom-waveguide coupling strength is characterized by the parameter β_n, defined as the ratio between the spontaneous emission rate of the nth atom into the considered waveguide mode and the total photon emission rate of a single atom into all modes, 2γ; see Fig. 1(b). Throughout this Letter, we assume unidirectional propagation, an approximation which is justified by the collective enhancement of forward emission typical of the timed Dicke state [2,10] and which holds as long as the atoms are not arranged at the Bragg condition (i.e., interatomic distance equal to an integer multiple of $(\lambda/2)$). In addition, for simplicity we also assume that all atoms have the same coupling strength β to the waveguide, a situation which describes well, e.g., trapped atoms [7,24,25]. However, our model can be easily extended to the general case, as shown in the Supplemental Material [26].

The general quantum state of the system can be written as

$$|\psi(t)\rangle = \left[\sum_{n=1}^{N} e^{ikz_n}\phi_n(t)\hat{\sigma}_n^+ + \int_{-\infty}^{\infty} e^{ikz_n}\chi(t,z)\hat{a}_z^\dagger dz\right]|0\rangle + |\psi_{fs}(t)\rangle, \quad (2)$$

where $\phi_n(t)$ and z_n represent the excited state amplitude and the position along the fiber of the nth atom in the ensemble, respectively. In addition, $\chi(t,z)$ indicates the complex amplitude of the waveguide-coupled light field, $\hat{a}_z^\dagger$ is the creation operator for a forward-propagating photon at position z, and $|\psi_{fs}(t)\rangle$ denotes the wave function associated with the field emitted in free space.

The collective decay rate of the ensemble, $\Gamma_{\text{ens}}(t)$ is defined as the ratio between the energy loss rate and the energy stored in the ensemble:

$$\Gamma_{\text{ens}}(t) = -\frac{\sum_{n=1}^{N}\frac{\partial}{\partial t}|\phi_n(t)|^2}{\sum_{n=1}^{N}|\phi_n(t)|^2} = \Gamma_{\text{fs}} + \Gamma_{\text{ens,wg}}(t), \quad (3)$$

where $\Gamma_{\text{fs}} = (1-\beta)2\gamma$ is the decay rate into free space, that we assume to be the same for all atoms. The second term, $\Gamma_{\text{ens,wg}}(t)$, indicates the ensemble decay rate into the waveguide, defined as the energy leaving the ensemble via guided light divided by the stored energy,

$$\Gamma_{\text{ens,wg}}(t) = \frac{v_g|\chi_N(t)|^2}{\sum_{n=1}^{N}|\phi_n(t)|^2}, \quad (4)$$

where $\chi_N(t)$ is the complex amplitude of the light field right after the Nth atom and v_g is the group velocity of the guided optical mode. We note that $\Gamma_{\text{ens}}(t)$ is sometimes inferred from the decay rate of the light intensity emitted by the atoms into the considered mode $\Gamma_{\text{light}}(t)$ [4,5,9,10,12], i.e.,

$$\Gamma_{\text{light}}(t) = -\frac{\partial}{\partial t}\left[\log\left(\frac{|\chi_N(t)|^2}{|\chi_N(0)|^2}\right)\right] = -\frac{\frac{\partial}{\partial t}|\sum_{n=1}^{N}\phi_n(t)|^2}{\sum_{n=1}^{N}|\phi_n(t)|^2}. \quad (5)$$

However, while convenient to access experimentally, a comparison between Eqs. (3) and (5) shows that this quantity is in general not related to $\Gamma_{\text{ens}}(t)$, whose estimation requires access to the complete state of the system. Interestingly, at $t=0$, Γ_{ens} and Γ_{light} coincide for the timed Dicke state (see Supplemental Material [26]).

To theoretically describe the time evolution of $|\psi(t)\rangle$, we follow the approach of Refs. [10,15,27], which, starting from a real-space Hamiltonian, allows us to calculate the excitation amplitudes ϕ_n in the steady state by solving the time-independent Schrödinger equation. In the low excitation limit, the dynamics of the system in the time domain can be then obtained via Fourier analysis (see Supplemental Material [26]).

For a system that is prepared in the timed Dicke state, i.e., $\phi_n(t=0) = 1/\sqrt{N}$, with $n = 1, \ldots, N$, and that then evolves freely, our model allows us to derive analytic expressions for $\phi_n(t)$ and $\chi_n(t)$, where the latter is proportional to the sum of the excited state amplitudes of the first n atoms:

$$\phi_n(t) = \frac{1}{\sqrt{N}} e^{-\gamma t} L_{n-1}^{(0)}(2\beta\gamma t), \tag{6}$$

$$\chi_n(t) = \frac{\sqrt{2\beta\gamma}}{i\sqrt{v_g}} \sum_{m=1}^{n} \phi_m(t) = \frac{\sqrt{2\beta\gamma}}{i\sqrt{v_g N}} e^{-\gamma t} L_{n-1}^{(1)}(2\beta\gamma t), \tag{7}$$

where $L_m^{(\alpha)}$ are the generalized Laguerre polynomials. The solutions show that, with the exception of the factor $e^{-\gamma t}$, the entire dynamics only depends on the product $\beta\gamma t$ and therefore it is essentially the same for any emitter-mode coupling strength β after appropriate scaling of the observation time. In the limit $\beta = 1$, these results agree with calculations based on a master equation approach [19].

Equations (6) and (7) completely determine the state of the system and allow one to calculate quantities of interest such as the total waveguide-coupled optical power $|\chi(t)|^2$ and $\Gamma_{\mathrm{ens}}(t)$, which, as an example, are shown in Figs. 2(a) and 2(b), respectively, for the case $N = 4$ and $\beta = 0.4$. At $t = 0$ the ensemble is in the timed Dicke state and exhibits a superradiant decay rate into the waveguide mode, which is N times enhanced with respect to the decay rate of a single atom: $\Gamma_{\mathrm{ens,wg}}(0) = 2\beta\gamma N$. For $t > 0$, unlike for the predictions of the standard Dicke model, the waveguide-coupled light power exhibits $N-1$ zeros, whose times of occurrence, τ_m $(m = 1, \ldots, N-1)$, are the roots of $L_{N-1}^{(1)}(2\beta\gamma t)$. This relation explicitly defines a set of states, which are subradiant with respect to the waveguide:

$$|\mathrm{sub}_m\rangle = \sum_{n=1}^{N} e^{ikz_n} \phi_n(\tau_m) \hat{\sigma}_n^{+} |0\rangle. \tag{8}$$

For these states, we have $\Gamma_{\mathrm{ens,wg}}(\tau_m) = 0$. However, the emission into free space is unmodified; therefore, $\Gamma_{\mathrm{ens}}(\tau_m) = \Gamma_{\mathrm{fs}}$, which is also the minimum total decay rate that can be obtained in the considered configuration; see Fig. 2(b). We note that Eq. (8) can also be used to construct the subradiant states of the traditional Dicke model by setting $z_n = 0$, for $i = 1, \ldots, N$.

Figure 2(c) shows the excited state amplitudes for the super- and subradiant states. For instance, for the first subradiant state $|\mathrm{sub}_1\rangle$, the first and last two atoms of the ensemble radiate in phase opposition, causing fully destructive interference of the waveguide-coupled light fields. The subsequent subradiant states are characterized by a similar structure, but the number of subensembles of consecutive atoms that radiate with opposite phases increases progressively by one. These states are all orthogonal to each other and to the timed Dicke state (i.e., the superradiant state). All together, these states form a complete basis of the subspace in which a single excitation is shared by the atoms, allowing a full description of the state of the ensemble (see Supplemental Material [26]). In Fig. 2(c), the phase differences are evaluated with respect to the phase of the first atom in the array.

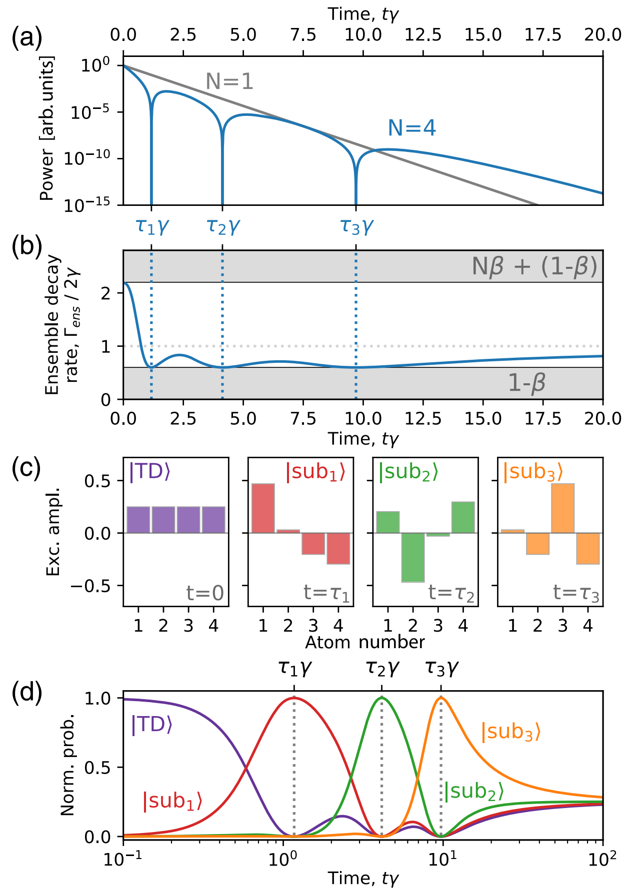

FIG. 2. (a) Calculated waveguide-coupled power $|\chi(t)|^2$ (normalized at $t = 0$) as a function of time for $N = 4$ atoms (blue line) with $\beta = 0.4$. For comparison, the case for $N = 1$ atom is shown as a gray line. (b) Ensemble decay rate $\Gamma_{\mathrm{ens}}(t)$ as a function of normalized time. The vertical blue dashed lines indicate the instants corresponding to which the ensemble is in a subradiant state with respect to the waveguide, $t = \tau_i$, $i = 1, 2, 3$. (c) Normalized excited state amplitude for the atoms in the ensemble for the timed Dicke state and the subradiant states. (d) Projection on the timed Dicke state and the subradiant states of the residual excitation stored in the ensemble as a function of time.

To shed further light on the system dynamics, Fig. 2(d) shows the decomposition onto this basis of the residual excitation stored in the atoms as a function of time. The ensemble, initially prepared in the timed Dicke state, passes through all the subradiant states and eventually remains (for $t \gg \tau_{N-1}$) in a superposition of the timed Dicke and the subradiant states with equal probability of $1/N$. At this point, $\Gamma_{\rm ens}(t)$ asymptotically converges to the single-atom decay rate, i.e., 2γ; see Fig. 2(b). This process remains qualitatively unaltered for any atom number N and coupling strength β.

It is interesting to note that for $\beta \ll 1$ and large N the time evolution of the ensemble becomes independent of the individual atom-mode coupling strength and only depends on the optical depth, $\mathrm{OD} \simeq 4\beta N$. Indeed, under these conditions, we can approximate Eqs. (6) and (7) as

$$\phi_n(t) \simeq \frac{1}{\sqrt{N}} e^{-\gamma t} J_0\left(\sqrt{2\gamma \mathrm{OD}\frac{n-1}{N}t}\right), \tag{9}$$

$$\chi_N(t) \simeq \frac{\sqrt{\mathrm{OD}}}{i\sqrt{4v_g\beta t}} e^{-\gamma t} J_1(\sqrt{2\gamma \mathrm{OD} t}), \tag{10}$$

where $J_\alpha(x)$ are the Bessel functions of the first kind (see Supplemental Material [26]). These relations are relevant for experiments involving large numbers of emitters and agree with results obtained for continuous resonant media [32]. The fact that the argument of the Bessel functions only depends on the OD suggests that the dynamics of the system is also well described by Eqs. (9) and (10) when the coupling strength varies from atom to atom as long as $\beta_n \ll 1$; see Fig. 1. We numerically confirmed that this is indeed the case.

In the one-dimensional geometry considered here, the timed Dicke state can be approximately prepared by exciting the atoms with very short laser pulses, carrying an average energy corresponding to less than one photon. However, this method is very inefficient because most of the time the excitation pulse passes through the ensemble without interacting with the atoms, complicating the observation of the atom-emitted light with good signal-to-noise ratio. To experimentally explore the concepts discussed above, we therefore preferred to employ long boxcar-shaped excitation pulses. They prepare a state, whose time dynamics has the same features as that of the timed Dicke state, but can be prepared with significantly higher probability; see Supplemental Material [26].

Figure 3(a) shows a sketch of the experimental setup. A single-mode optical nanofiber with a 400-nm diameter and a waist length of 1 cm is placed in a vacuum chamber and surrounded by a cloud of cold Cs atoms from a magneto-optical trap. Nanofiber-guided excitation pulses that are near-resonant with the Cs D2 transition ($6S_{1/2}$, $F = 4 \to 6P_{3/2}$, and $F' = 5$) are generated from an incident cw laser beam using an electro-optic modulator followed by an acousto-optic modulator. The < 1-ns fall time (90%–10%) of the pulses is much shorter than the lifetime of the excited state ($\tau = 1/2\gamma = 30.4$ ns, $\gamma/2\pi = 2.6$ MHz [33]), while the total pulse length (100 ns $> 3\tau$) is long enough for the system to approximately reach a steady state. The optical power transmitted through the nanofiber is measured using a

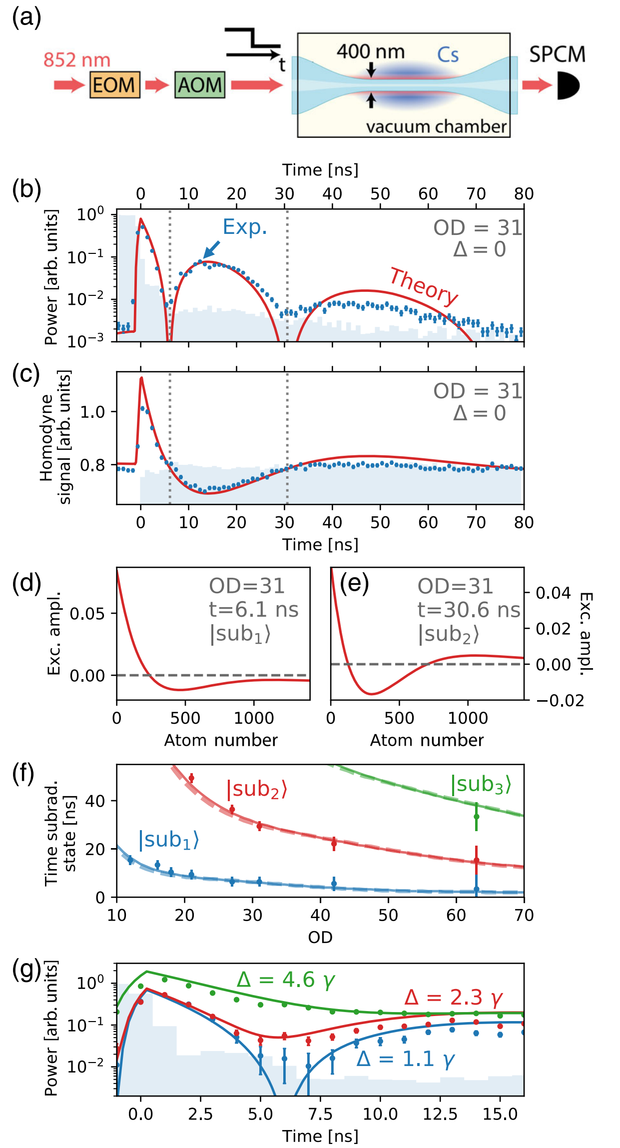

FIG. 3. (a) Experimental setup. Cs, cesium; EOM, electro-optic modulator; AOM, acousto-optic modulator; SPCM, single-photon counting module. (b) Measured (blue dots) and predicted (red line) optical power exiting the nanofiber for $\Delta = 0$ and $\mathrm{OD} = 31$. The blue shaded area shows the measured pulse obtained using the same experimental sequence, but in the absence of atoms. (c) Measured (blue dots) and predicted (red line) homodyne signal between the atom-emitted light and a local oscillator for the same parameters as in (b). (d),(e) Calculated excited state amplitudes of each atom for the parameters as in (b) for the first (d) and second (e) subradiant state. These states are reached at $t = 6.1$ ns and $t = 30.6$ ns, as indicated in (b) and (c) with dashed gray lines. (f) Time at which the system reaches the first (blue line and dots), second (red line and dots), and third (green line and dot) subradiant state as a function of the OD. The measurements for OD of 42 and 63 have been obtained with 2 and 3 passes of the pulse through the ensemble, respectively; see Supplemental Material [26]. The dots are measured data, while the solid and dashed lines are theoretical predictions for $\beta = 0.55\%$ and $\beta = 20\%$, respectively. (g) Measured optical power for $\mathrm{OD} = 28$ and $\Delta = 1.1\gamma$ (blue dots), $\Delta = 2.3\gamma$ (red dots), and $\Delta = 4.6\gamma$ (green dots). The solid lines are theoretical predictions.

single-photon counting module. We note that each excitation pulse has a mean power significantly smaller than one single-photon energy per atomic lifetime. This ensures that, on average, less than one excitation is stored in the atomic ensemble.

Time-resolved measurements of the emitted optical power are shown in Fig. 3(b) for probe pulses resonant with the atomic transition, i.e., detuning $\Delta = \omega - \omega_a = 0$, where $\omega_a = 0$ is the atomic resonance frequency, and for $\mathrm{OD} = 31 \pm 1$. The OD is estimated by fitting our theoretical model to the data and is the only fit parameter. The error represents the 99% confidence intervals from the fit. Right after the switch-off of the excitation pulse at $t = 0$, the ensemble initially decays at a superradiant rate, reaching minima in transmission around $t = 6.1$ ns and $t = 30.6$ ns. Figures 3(d) and 3(e) depict the calculated excited state amplitudes for the atoms in the ensemble at these moments in time. Complete destructive interference of the light emitted from atoms into the guided mode is predicted; i.e., the ensemble is in a subradiant state with respect to the nanofiber-guided mode.

Our theoretical model predicts a change in the sign of the projection of the ensemble state on the timed Dicke state and thus of the emitted light field amplitude each time the system passes through one of the subradiant states. To experimentally investigate this feature, we repeat the measurement of Fig. 3(b), this time interfering the light emitted by the atomic ensemble with a local oscillator. The result is shown in Fig. 3(c), in which clear constructive and destructive interference with the local oscillator is observed before and after the first subradiant state, respectively, in very good agreement with our predictions.

Figure 3(f) illustrates the time at which the system is in the first (blue points and lines), second (red points and lines), and third (green point and lines) subradiant state as a function of the OD. The theoretical predictions shown as solid lines have been calculated for $\beta = 0.55\% \pm 0.13\%$, which is the average value measured in our experiment [30], while the dashed lines correspond to a much larger value of $\beta = 20\%$ (approximately the highest β that can be achieved in a nanofiber atom interface [31]). The close agreement between the two theory predictions and the experimental data confirms that for $N \gg 1$ the time evolution of the system depends on OD rather than on atom number.

Excitation via moderately detuned laser pulses results in an additional phase shift between subsequent atoms due to the dispersive response of the ensemble, which prevents complete destructive interference of the collective emission. This was experimentally investigated by launching into the nanofiber pulses, whose central frequency is detuned with respect to the atomic transition. The results are shown in Fig. 3(g), in which the transmitted power for a time interval close to when the system reaches the first subradiant state is depicted for several detunings Δ. As expected, compared to the case $\Delta = 0$, larger detunings cause a gradual disappearance of the first minimum in the transmitted optical power.

In conclusion, we have shown that an ensemble of N emitters prepared in the timed Dicke state with respect to a given propagating mode evolves through $N - 1$ subradiant states. This results in aperiodic switch-offs of the collectively emitted optical power. This nonmonotonous decay originates from the dynamics induced by atom-atom coupling via propagating photons. Our predictions are in excellent agreement with power and phase-sensitive measurements of the light emitted by an ensemble of Cs atoms coupled to the guided mode of an optical nanofiber. Beyond providing fundamental insight into collective atom-light coupling, our results are of direct relevance for systems whose dynamics involve timed Dicke states as, e.g., optical quantum memories [34,35] and atomic ensembles in cavity and waveguide quantum electrodynamics [7,30,36].

We acknowledge financial support by the Alexander von Humboldt Foundation in the framework of an Alexander von Humboldt Professorship endowed by the Federal Ministry of Education and Research and by the Austrian Science Fund (NanoFiRe grant Project No. P31115).

*riccardo.pennetta@hu-berlin.de
†juergen.volz@hu-berlin.de

[1] R. H. Dicke, Coherence in spontaneous radiation processes, Phys. Rev. **93**, 99 (1954).

[2] M. O. Scully, E. S. Fry, C. H. R. Ooi, and K. Wódkiewicz, Directed Spontaneous Emission from an Extended Ensemble of N Atoms: Timing is Everything, Phys. Rev. Lett. **96**, 010501 (2006).

[3] M. O. Araújo, I. Krešić, R. Kaiser, and W. Guerin, Superradiance in a Large and Dilute Cloud of Cold Atoms in the Linear-Optics Regime, Phys. Rev. Lett. **117**, 073002 (2016).

[4] S. Roof, K. Kemp, M. Havey, and I. Sokolov, Observation of Single-Photon Superradiance and the Cooperative Lamb Shift in an Extended Sample of Cold Atoms, Phys. Rev. Lett. **117**, 073003 (2016).

[5] W. Guerin, M. O. Araújo, and R. Kaiser, Subradiance in a Large Cloud of Cold Atoms, Phys. Rev. Lett. **116**, 083601 (2016).

[6] G. Ferioli, A. Glicenstein, L. Henriet, I. Ferrier-Barbut, and A. Browaeys, Storage and Release of Subradiant Excitations in a Dense Atomic Cloud, Phys. Rev. X **11**, 021031 (2021).

[7] A. Goban, C.-L. Hung, J. Hood, S.-P. Yu, J. Muniz, O. Painter, and H. Kimble, Superradiance for Atoms Trapped Along a Photonic Crystal Waveguide, Phys. Rev. Lett. **115**, 063601 (2015).

[8] S. Okaba, D. Yu, L. Vincetti, F. Benabid, and H. Katori, Superradiance from lattice-confined atoms inside hollow core fibre, Commun. Phys. **2**, 136 (2019).

[9] R. J. Bettles, T. Ilieva, H. Busch, P. Huillery, S. W. Ball, N. L. R. Spong, and C. S. Adams, Collective mode interferences in light-matter interactions, arXiv:1808.08415v4.

[10] R. Pennetta, M. Blaha, A. Johnson, D. Lechner, P. Schneeweiss, J. Volz, and A. Rauschenbeutel, Collective Radiative Dynamics of an Ensemble of Cold Atoms Coupled to an Optical Waveguide, Phys. Rev. Lett. **128**, 073601 (2022).
[11] A. Paris-Mandoki, C. Braun, J. Kumlin, C. Tresp, I. Mirgorodskiy, F. Christaller, H. P. Büchler, and S. Hofferberth, Free-Space Quantum Electrodynamics with a Single Rydberg Superatom, Phys. Rev. X **7**, 041010 (2017).
[12] N. Stiesdal, H. Busche, J. Kumlin, K. Kleinbeck, H. P. Büchler, and S. Hofferberth, Observation of collective decay dynamics of a single Rydberg superatom, Phys. Rev. Research **2**, 043339 (2020).
[13] R. Röhlsberger, K. Schlage, B. Sahoo, S. Couet, and R. Rffer, Collective Lamb shift in single-photon superradiance, Science **328**, 1248 (2010).
[14] M. Tavis and F. W. Cummings, Exact solution for an N-molecule-radiation-field hamiltonian, Phys. Rev. **170**, 379 (1968).
[15] M. Blaha, A. Johnson, A. Rauschenbeutel, and J. Volz, Beyond the tavis-cummings model: Revisiting cavity QED with ensembles of quantum emitters, Phys. Rev. A **105**, 013719 (2022).
[16] Y. Colombe, T. Steinmetz, G. Dubois, F. Linke, D. Hunger, and J. Reichel, Strong atom–field coupling for Bose–Einstein condensates in an optical cavity on a chip, Nature (London) **450**, 272 (2007).
[17] F. Brennecke, T. Donner, S. Ritter, T. Bourdel, M. Khl, and T. Esslinger, Cavity QED with a Bose–Einstein condensate, Nature (London) **450**, 268 (2007).
[18] A. A. Svidzinsky, J. T. Chang, and M. O. Scully, Dynamical Evolution of Correlated Spontaneous Emission of a Single Photon from a Uniformly Excited Cloud of N Atoms, Phys. Rev. Lett. **100**, 160504 (2008).
[19] J. Kumlin, K. Kleinbeck, N. Stiesdal, H. Busche, S. Hofferberth, and H. P. Büchler, Nonexponential decay of a collective excitation in an atomic ensemble coupled to a one-dimensional waveguide, Phys. Rev. A **102**, 063703 (2020).
[20] H. H. Jen, M.-S. Chang, G.-D. Lin, and Y.-C. Chen, Subradiance dynamics in a singly excited chirally coupled atomic chain, Phys. Rev. A **101**, 023830 (2020).
[21] P. R. Berman, Theory of two atoms in a chiral waveguide, Phys. Rev. A **101**, 013830 (2020).
[22] V. A. Pivovarov, L. V. Gerasimov, J. Berroir, T. Ray, J. Laurat, A. Urvoy, and D. V. Kupriyanov, Single collective excitation of an atomic array trapped along a waveguide: A study of cooperative emission for different atomic chain configurations, Phys. Rev. A **103**, 043716 (2021).
[23] F. Le Kien and A. Rauschenbeutel, Nanofiber-mediated chiral radiative coupling between two atoms, Phys. Rev. A **95**, 023838 (2017).
[24] E. Vetsch, D. Reitz, G. Sagué, R. Schmidt, S. T. Dawkins, and A. Rauschenbeutel, Optical Interface Created by Laser-Cooled Atoms Trapped in the Evanescent Field Surrounding an Optical Nanofiber, Phys. Rev. Lett. **104**, 203603 (2010).
[25] J. D. Thompson, T. G. Tiecke, N. P. de Leon, J. Feist, A. V. Akimov, M. Gullans, A. S. Zibrov, V. Vuletic, and M. D. Lukin, Coupling a single trapped atom to a nanoscale optical cavity, Science **340**, 1202 (2013).
[26] See Supplemental Material at http://link.aps.org/supplemental/10.1103/PhysRevLett.128.203601 for more details on (1) the theoretical model, (2) initial ensemble decay rate and pulse decay rate for the timed Dicke state, (3) ensemble state prepared in the experiment and theoretical solutions for this case, (4) approximation for $N \gg 1$ and $\beta \ll 1$, (5) assumptions of the theoretical model and their validity in the experiment, (6) orthogonality of the subradiant states, (7) experimental sequence, and (8) interference with local oscillator, which includes Refs. [27–31].
[27] J.-T. Shen and S. Fan, Theory of single-photon transport in a single-mode waveguide. I. coupling to a cavity containing a two-level atom, Phys. Rev. A **79**, 023837 (2009).
[28] P. Lodahl, S. Mahmoodian, S. Stobbe, A. Rauschenbeutel, P. Schneeweiss, J. Volz, H. Pichler, and P. Zoller, Chiral quantum optics, Nature (London) **541**, 473 (2017).
[29] D. Reitz, C. Sayrin, B. Albrecht, I. Mazets, R. Mitsch, P. Schneeweiss, and A. Rauschenbeutel, Backscattering properties of a waveguide-coupled array of atoms in the strongly nonparaxial regime, Phys. Rev. A **89**, 031804(R) (2014).
[30] A. Johnson, M. Blaha, A. E. Ulanov, A. Rauschenbeutel, P. Schneeweiss, and J. Volz, Observation of Collective Superstrong Coupling of Cold Atoms to a 30-m Long Optical Resonator, Phys. Rev. Lett. **123**, 243602 (2019).
[31] F. L. Kien, S. D. Gupta, V. I. Balykin, and K. Hakuta, Spontaneous emission of a cesium atom near a nanofiber: Efficient coupling of light to guided modes, Phys. Rev. A **72**, 032509 (2005).
[32] U. van Bürck, Coherent pulse propagation through resonant media, Hyperfine Interact. **123/124**, 483 (1999).
[33] D. Steck, Cesium d line data, http://steck.us/alkalidata.
[34] A. I. Lvovsky, B. C. Sanders, and W. Tittel, Optical quantum memory, Nat. Photonics **3**, 706 (2009).
[35] C. Simon *et al.*, Quantum memories, Eur. Phys. J. D **58**, 1 (2010).
[36] F. Mivehvar, F. Piazza, T. Donner, and H. Ritsch, Cavity QED with quantum gases: New paradigms in many-body physics, Adv. Phys. **70**, 1 (2021).